

Characterization and modeling of antireflective coatings of Si O₂, Si₃N₄, and Si O_xN_y deposited by electron cyclotron resonance enhanced plasma chemical vapor deposition

S. N. M. Mestanza, M. P. Obrador, E. Rodriguez, C. Biasotto, I. Doi, J. A. Diniz, and J. W. Swart

Citation: *Journal of Vacuum Science & Technology B* **24**, 823 (2006); doi: 10.1116/1.2181577

View online: <http://dx.doi.org/10.1116/1.2181577>

View Table of Contents: <http://scitation.aip.org/content/avs/journal/jvstb/24/2?ver=pdfcov>

Published by the AVS: Science & Technology of Materials, Interfaces, and Processing

Articles you may be interested in

[Crystallization of Si₃N₄ layers and its influences on the microstructure and mechanical properties of ZrN/Si₃N₄ nanomultilayers](#)

Appl. Phys. Lett. **89**, 121916 (2006); 10.1063/1.2348092

[Surface evolution of nanostructured CrN and Si₃N₄ films](#)

J. Appl. Phys. **94**, 6827 (2003); 10.1063/1.1617358

[Atomic structure analysis of SiO₂/Si and Si₃N₄/Si interfaces by high-resolution transmission electron microscopy](#)

J. Vac. Sci. Technol. A **21**, 495 (2003); 10.1116/1.1554951

[Interaction of a Ti-capped Co thin film with Si₃N₄](#)

Appl. Phys. Lett. **77**, 4307 (2000); 10.1063/1.1329329

[A Knudsen effusion mass spectrometric study of the molecule Si₃N](#)

J. Chem. Phys. **106**, 6016 (1997); 10.1063/1.473610



Instruments for Advanced Science

<p>Contact Hiden Analytical for further details: W www.HidenAnalytical.com E info@hiden.co.uk</p> <p>CLICK TO VIEW our product catalogue</p>	 <p>Gas Analysis</p> <ul style="list-style-type: none"> › dynamic measurement of reaction gas streams › catalysis and thermal analysis › molecular beam studies › dissolved species probes › fermentation, environmental and ecological studies 	 <p>Surface Science</p> <ul style="list-style-type: none"> › UHV TPD › SIMS › end point detection in ion beam etch › elemental imaging - surface mapping 	 <p>Plasma Diagnostics</p> <ul style="list-style-type: none"> › plasma source characterization › etch and deposition process reaction › kinetic studies › analysis of neutral and radical species 	 <p>Vacuum Analysis</p> <ul style="list-style-type: none"> › partial pressure measurement and control of process gases › reactive sputter process control › vacuum diagnostics › vacuum coating process monitoring
---	--	--	--	--

Characterization and modeling of antireflective coatings of SiO_2 , Si_3N_4 , and SiO_xN_y deposited by electron cyclotron resonance enhanced plasma chemical vapor deposition

S. N. M. Mestanza^{a)}

Universidade Estadual de Campinas, Centro de Componentes Semicondutores, P.O. Box 6061, CEP 13083-970 Campinas, SP, Brazil

M. P. Obrador

Universidade de Girona, EPS, Avenida Lluís Santaló s/n (Campus de Montilivi), 17071 Girona, Spain

E. Rodriguez

Universidade Estadual de Campinas, Instituto de Fisica "Gleb-Wataghin," Departamento de Eletrônica Quântica, P.O. Box 6165, CEP 13084-970 Campinas, SP, Brazil

C. Biasotto, I. Doi, J. A. Diniz, and J. W. Swart

Universidade Estadual de Campinas, Centro de Componentes Semicondutores, P.O. Box 6061, CEP 13083-870 Campinas, SP, Brazil

(Received 26 July 2005; accepted 6 February 2006; published 24 March 2006)

In this work the optical transmission spectra of silicon oxide (SiO_2), silicon nitrides (Si_3N_4), silicon-rich oxynitrides (SiO_xN_y), and antireflective coatings (ARCs), deposited by the electron cyclotron resonance enhanced plasma chemical vapor deposition onto a silicon substrate at room temperature, are studied. Simulations carried out with the MATHEMATICA program, from 0 to 1000 nm thick coatings, showed maximum transmittance in the three basic colors at 620, 480, and 560 nm for the SiO_2 , Si_3N_4 , and SiO_xN_y ARCs, respectively. However, a highly significant transmittance over a broad spectral range from visible (VIS) to near the infrared region, with optical gain in the three basic colors above 20%, is observed only at thicknesses of 80, 70, and 60 nm, respectively, for SiO_2 , Si_3N_4 , and SiO_xN_y ARCs. Among the three evaluated films, the highest transmittance in the broad spectral band in the VIS range was observed for 60 nm thick Si_3N_4 films. The Fourier transform infrared spectroscopy of these films reveal high structural quality and the presence of Si–O, Si–H, N–H, and Si–N bonds, independent of thickness and deposition parameters. © 2006 American Vacuum Society. [DOI: 10.1116/1.2181577]

I. INTRODUCTION

The sensitivity improvement of active pixel sensors (APS) is one of the main issues related to their applications as image sensors. In this sense, the aim of this work is to address the enhancement of the transmittance in order to optimize the APS device sensitivity. Presently, the main disadvantage of APS in comparison to the charge coupled devices¹ (CCD) is APS low resolution when used in image sensor applications. APS sensors have the advantages, however, of low power consumption, low costs, and high integrability. On the other hand, nowadays the tendency to increase the number of the pixels, reducing their size on the same chip, leads unavoidably to the signal-to-noise ratio² decreasing problem. One simple solution to overcome this problem is the use of a single top layer [such as an antireflective coating (ARC)] on the photodetector devices. In this case, the matching between the antireflective coatings and semiconductor's refractive index becomes of crucial importance in order to achieve acceptable performance. The antireflective coating also passivates the surface of the semiconductor, i.e., minimizes the density of interface states.

Due to the existence of the excellent interface between Si and SiO_2 , the transmittance of this material is used as a reference to compare this parameter to the other films that are compatible with complementary metal oxide semiconductor (CMOS) processes. In order to evaluate the results predicted by the simulations of light transmittance into the Si substrate, different types of ARCs were deposited employing an electron cyclotron resonance enhanced plasma chemical vapor deposition (ECR-CVD).³

This work focuses on the optimization of the ARCs' thicknesses on the transmittance of the the three basic colors, envisaging the development of a color sensor manufacturing process. Carrying out simulations it was possible to predict the type of material and the optimal thickness in relation to the obtained maximum transmittance. Therefore, the objective is to achieve a high transmittance on a broad visible (VIS) and near infrared (NIR) spectral range. The selected materials were SiO_2 , Si_3N_4 , and SiO_xN_y , all compatible with the CMOS process, in order to allow an assumable total cost.

II. TRANSMITTANCE MODEL

For ARC simulations, the following considerations were assumed: coatings are homogeneous, nonabsorbent, isotro-

^{a)}Author to whom correspondence should be addressed; electronic mail: nilo@led.unicamp.br

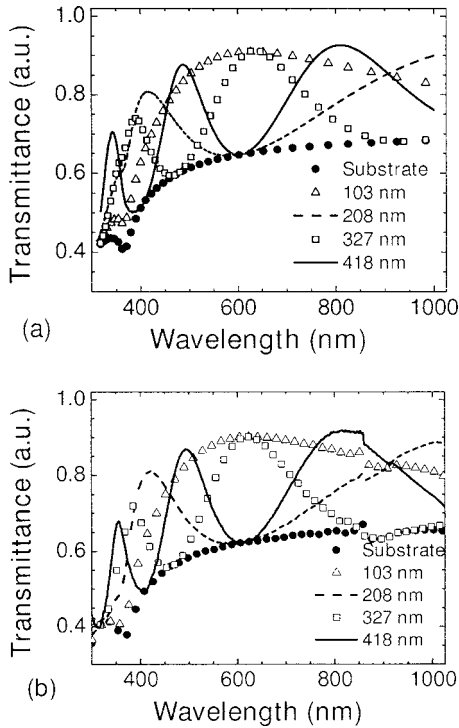


FIG. 1. Transmittance of the SiO_2 films as a function of wavelength for different film thicknesses: (●) substrate; (△) 103 nm; (---) 208 nm; (□) 327 nm; and (—) 418 nm. (a) Simulated and (b) measured.

pic, and with uniform thickness. Furthermore, the incidence of photons was assumed to be normal to the sample surface.

For normal incidence ($\phi_k=0$), the phase shift (δ_k) can be expressed by Eq. (1) (Refs. 4 and 5) when the light goes through an ARC of thickness (d_k) and refractive index n_k ,

$$\delta_k(\lambda) = \frac{2\pi}{\lambda_o} n_k(\lambda) d_k, \quad (1)$$

where λ_o is the vacuum wavelength.

The characteristic matrix for the wave propagation across a medium k is described by Eq. (2),

$$M_{\text{tot}}(\lambda) = \prod_{k=1}^m \begin{bmatrix} \cos \delta_k(\lambda) & (-i/n_k) \sin \delta_k(\lambda) \\ -i n_k \sin \delta_k(\lambda) & \cos \delta_k(\lambda) \end{bmatrix} = \begin{bmatrix} A & B \\ C & D \end{bmatrix}, \quad (2)$$

where the index m is the number of ARCs.

Knowing the elements of the matrix $M_{\text{tot}}(\lambda)$, A , B , C , and D , the transmission coefficient of the light on the ARCs can be determined by Eq. (3),

$$t = \frac{2n_o}{An_o + Bn_s n_o + Cn_o + D}, \quad (3)$$

where n_o and n_s are the values of refractive index for the air and the substrate, respectively.

Finally, the transmittance of the light to the Si substrate can be calculated as

$$T_{\text{tot}}(\lambda) = \frac{\text{Re}(n_{\text{Si}}(\lambda))}{n_o} |t|^2. \quad (4)$$

III. EXPERIMENT

A. Sample preparation

SiO_2 , Si_3N_4 , and SiO_xN_y thin films were deposited using Plasma-Therm SLR 770 ECR-CVD system. This system uses 100–1000 W microwave power at 2.45 GHz. The ionization and extraction magnet current was set to 180 and 0 A, respectively. The ion energy was controlled with a radio frequency (rf) power supply (0–140 W, 13.56 MHz). The films were grown on an n -type, (100), Si substrate with resistivity of $\sim 2.6 \Omega \text{ cm}$ at room temperature. The substrate temperature was always kept at 20 °C. The processing parameters used in these experiments were 200 SCCM (standard cubic centimeter per minute) $\text{SiH}_4/40$ SCCM $\text{O}_2/20$ SCCM Ar/15 mtorr pressure/950 W ECR/3 W rf/20 °C and ~ -3 V dc bias to obtain the SiO_2 films; 200 SCCM $\text{SiH}_4/7$ SCCM $\text{N}_2/13$ SCCM $\text{O}_2/20$ SCCM Ar/5 mtorr pressure/950 W ECR/5 W rf/20 °C and ~ -3 V dc bias, for the SiO_xN_y films; and 200 SCCM $\text{SiH}_4/5$ SCCM $\text{N}_2/20$ SCCM Ar/5 mtorr pressure/950 W ECR/5 W rf/20 °C and ~ -3 V dc bias for the Si_3N_4 films. The deposition rates were 13, 20, and 19 nm/min, for the SiO_2 , SiO_xN_y , and Si_3N_4 films, respectively.

B. Measurement techniques

Because of the high absorbance of the Si substrate in the range of 400–1100 nm wavelengths and due to the fact that the studied films are transparent within this range, the transmittance (T) was obtained by the relation $T+R=1$. The measurements of the total reflectance (R) were accomplished by an integrating sphere using a Lambda 9 Perkin Elmer spectrophotometer, which operates in the 200–3200 nm range.

The refractive index and thickness of the films was measured using a Rudolph Research Auto EL-II automatic ellipsometer, on $\lambda=632.8$ nm at 70° incidence. Since ARC, thickness, and refractive index values are the critical parameters for the transmittance evaluation, the thickness measurements were double checked using another measurement device [a Rudolph/Fourier transform method (FTM) interferometer], with excellent agreement in the results. Moreover, to assure film uniformity, the measurements of the thickness (d) and refractive index (n) of the ARCs were taken on several different points over the whole surface of the samples.

C. Simulations

In order to evaluate the experimental results, the transmittance of antireflective coatings SiO_2/Si , $\text{Si}_3\text{N}_4/\text{Si}$, and $\text{SiO}_x\text{N}_y/\text{Si}$ were also simulated using the MATHEMATICA program. Simulations were carried out for the ARCs with the same thickness in the spectral range (300–1000 nm) used for transmittance measurements. The experimental values obtained for n_k and d_k were used to perform the simulations of the SiO_2 , Si_3N_4 , and SiO_xN_y films. Because these films ex-

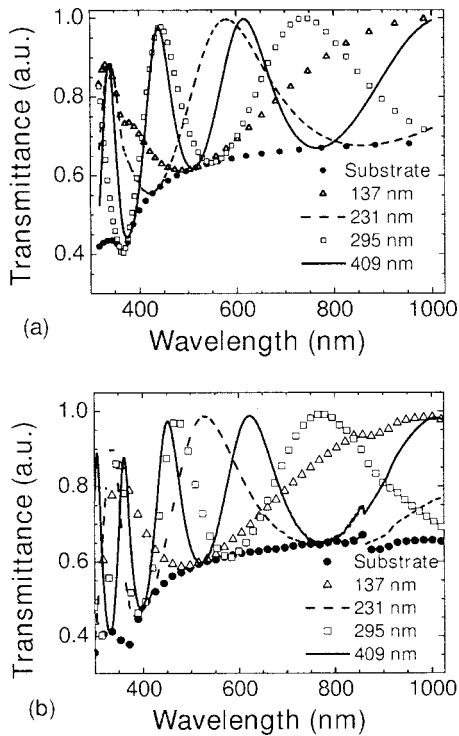


FIG. 2. Transmittance of the Si_3N_4 films as a function of wavelength for various thicknesses: (●) substrate; (△) 137 nm; (---) 231 nm; (□) 295 nm; and (—) 409 nm. (a) Simulated and (b) measured.

hibit low absorption through the considered spectral region, the value of the refractive index was assumed constant ($n_{\text{SiO}_2} = 1.46$; $n_{\text{Si}_3\text{N}_4} = 1.88$; $n_{\text{SiO}_x\text{N}_y} = 1.6$). For the refractive index of the Si substrate the value obtained by Edwards⁶ was used.

IV. EXPERIMENTAL RESULTS

A. Simulation and measurements of ARCs transmittance

In order to evaluate the increase of the films' transmittance in relation to the substrate (gain), we have considered the transmittance values at three basic colors: blue (B), green (G), and red (R), which are important for the color sensors' developments.

Figure 1(a) shows the results of simulated transmittance in SiO_2 films as a function of wavelength for different SiO_2 thicknesses. It can be clearly seen that the transmittance of the ARCs has a strong dependence on the wavelength of the incident light, as well as on the thickness of ARCs. The losses of light in the SiO_2/Si interface are between 30% and 60%. It can also be observed that for all the ARCs, the transmittance on the whole spectral range from VIS to NIR is always higher than the substrate one. This increase in transmittance is an attractive feature for the improvement of the quantum efficiency of sensor devices. Furthermore, by increasing the film thickness, an increase in the number of maxima and minima is observed related to multiple interferences. It must be pointed out that we are not interested in samples that have interference effects. It is desirable to ob-

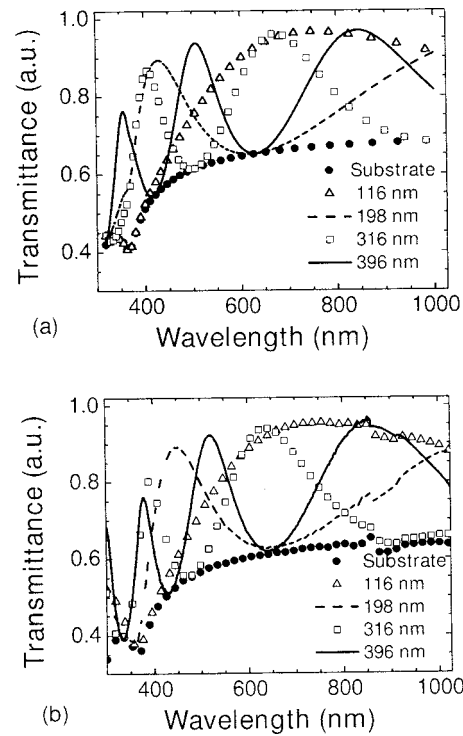


FIG. 3. Transmittance of the SiO_xN_y films as a function of wavelength for various thickness: (●) substrate; (△) 116 nm; (---) 198 nm; (□) 316 nm; and (—) 396 nm. (a) Simulated and (b) measured.

tain a high and approximately constant transmittance along the whole VIS and NIR range. For the lowest thickness of 103 nm, the gain values observed at the three basic colors are $B \sim 14\%$, $G \sim 27\%$, and $R \sim 26\%$.

Figure 1(b) shows the experimental measurements' result of transmittance in ARC layers of SiO_2 . This result is in good agreement with the ARCs' simulation results presented in Fig. 1(a). According to this result, for $d = 103$ nm a relatively large transmittance on a broad spectral range (400–1000 nm) is observed. The small perturbations observed on transmittance at 860 nm are due to the spectrometer automatic detector exchange switch.

Figure 2(a) shows the results of simulated transmittance in films of Si_3N_4 as a function of wavelength for different Si_3N_4 thicknesses. Figure 2(b) shows the experimental measurements of the transmittance of these Si_3N_4 films. An increase in the transmittance peak is observed in comparison to the SiO_2 films. For the lowest thickness (137 nm), the gains obtained are blue $\sim 18\%$, green $\sim 2\%$, and red $\sim 18\%$.

Figure 3(a) shows the results of simulated transmittance in films of SiO_xN_y , as a function of wavelength, for different thicknesses of SiO_xN_y . Figure 3(b) shows the experimental results of the transmittance in films of SiO_xN_y . The observed spectra are very similar and the number of maxima and minima lower, in comparison to those obtained for the SiO_2 films. The best behavior is achieved for the lowest thicknesses. For the lowest thickness (116 nm), the approximate gain value for the three basic colors, blue, green, and red, are $\sim 2\%$, $\sim 18\%$, and $\sim 24\%$, respectively.

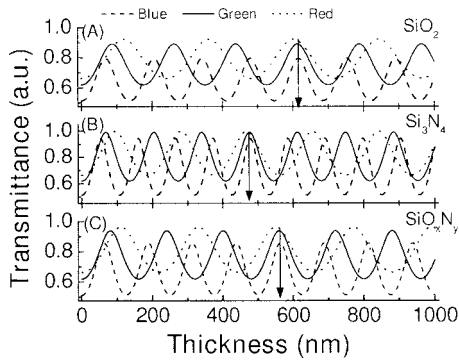


FIG. 4. Simulated transmittance spectra of (A) SiO_2 , (B) Si_3N_4 , and (C) SiO_xN_y films as a function of the thickness for the three basic colors, blue, green, and red. The arrows indicate the thicknesses, values in which a maximum transmittance was simultaneously achieved for all three basic colors.

Figure 4 shows the simulated transmittance spectra for three ARCs as a function of the thickness in the 0–1000 nm wavelength range. The results show that for each film, there is only one thickness that yields a high value of transmittance simultaneously at the three basic wavelengths. The thickness values that attain this transmittance are 620, 480, and 560 nm for the SiO_2 , Si_3N_4 , and SiO_xN_y coatings, respectively. The observed bandwidth for all three coatings is nearly 80 nm. However (again from Fig. 4) it can also be observed that for the three ARCs studied, there is a thinner ARC, for which the transmittance values at the three basic colors exhibit a maximum which is lower than that for the above cited thicknesses.

Figure 5 shows the optimized transmittances for the Si_3N_4 , SiO_xN_y , and SiO_2 ARCs as functions of the wavelength obtained for thicknesses of 60, 70, and 80 nm, respectively. The spectra show significantly high transmittance over a broad spectral range of 400–1000 nm (VIS and NIR). The Si_3N_4 films show the highest transmittance with optical gain in relation to the substrate at the three basic colors of blue (~40%), green (~35%), and red (~21%).

B. Optical properties of the ARCs

In order to study the internal structure of the ARC, the Fourier transform infrared (FTIR) technique was used. A

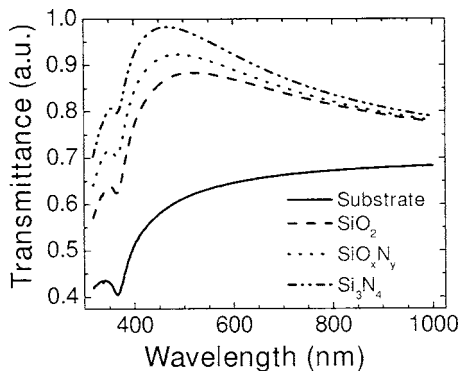


FIG. 5. Optimized transmittances for the Si_3N_4 , SiO_xN_y , and SiO_2 ARCs as function of the wavelength: (—) substrate; (---) SiO_2 ; (···) SiO_xN_y ; and (-·-·-) Si_3N_4 .

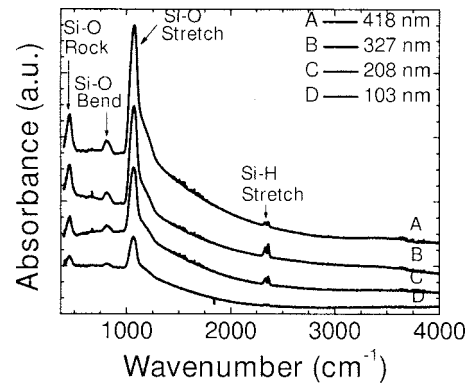


FIG. 6. FTIR absorbance spectra of optical films of SiO_2 .

common feature observed in all spectra is the increase of the peak intensity as the film thickness is increased, which agrees with the reports found in the literature.⁷

Figure 6 shows the FTIR absorbance spectra of SiO_2 films obtained for different film thicknesses. All the samples exhibit a noticeable absorption peak at $\sim 1080 \text{ cm}^{-1}$, which is attributed to the symmetric and asymmetric stretching vibrations of Si–O groups.^{8,9} Si–O rocking vibration is also common to all the samples and is observed at $\sim 452 \text{ cm}^{-1}$.¹⁰ Another interesting feature is the Si–H symmetric stretching vibration observed for all samples as a doublet band at 2235 and 2361 cm^{-1} .^{10,11} Furthermore the Si–O–Si bending mode is observed at 811 cm^{-1} .¹²

Figure 7 shows the FTIR absorbance spectra of Si_3N_4 films. The spectra mainly exhibit three absorption peaks. The first one is located at $\sim 475.7 \text{ cm}^{-1}$ and is related to the Si–N breathing.¹³ The second one located at $\sim 845.6 \text{ cm}^{-1}$ is associated to the Si–N stretching mode. The last one, related to the Si–H stretching mode, is a doublet band peak at 2336 and 2361 cm^{-1} , respectively.¹⁴ Two relatively weak peaks can be observed at ~ 668 and 3336.6 cm^{-1} , both related to the Si–H rocking and N–H stretching, respectively.^{9,10}

Figure 8 shows the FTIR absorbance spectrum for SiO_xN_y films of different thicknesses. Two strong absorption peaks located at 450 and 1008 cm^{-1} are typical for the Si–O rocking and stretching, respectively. Similar to the case of the SiO_2 , the absorption spectra of the SiO_xN_y also shows the main Si–H stretching vibration absorption peak as a doublet

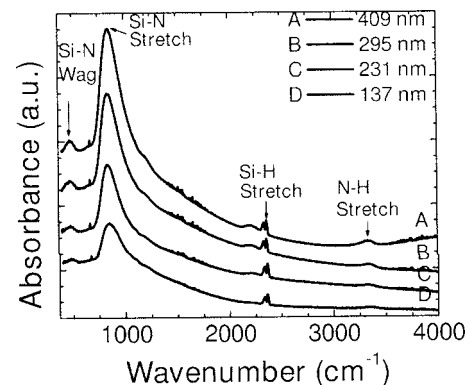


FIG. 7. FTIR absorbance spectra of optical films of Si_3N_4 .

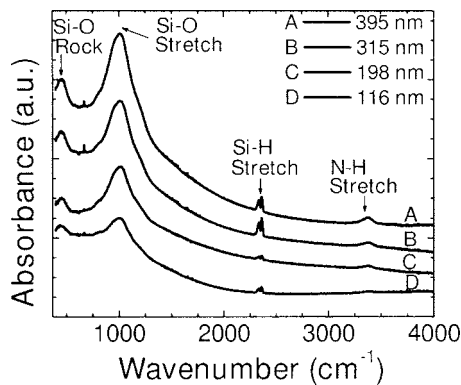


FIG. 8. FTIR absorbance spectra of optical films of SiO_xN_y .

band peak at 2339 and 2364 cm^{-1} . The weak peak observed at 3380 cm^{-1} is related to the N–H stretching mode.¹⁵

V. DISCUSSION OF RESULTS

The ARCs produce a diminution in the refractive index difference at the silicon-air interface, yielding an increase of the transmittance values both in measured and simulated results.

In all cases, the ARCs showed degradation in the optical properties in the ultra violet (UV) region. It can be attributed to the ARCs' rapid increase in the refractive index. Measured and simulated results show that (depending on the wavelength and the film thickness) 10%–40% of the incident light may be lost as the consequence of the reflection. This light reduction causes a reduction in the number of photocarriers, thus the quantum efficiency decrease of the sensor.

An interesting characteristic observed from the simulated results in the three ARCs is that by increasing the thickness, the maximum transmittance value shifts to higher wavelengths. In all the ARCs, it was observed that the number of transmittance peaks within the VIS and NIR spectrum increases by increasing the film thickness. This effect can be explained from the point of view of the interference of the electromagnetic wave in the ARCs.

In Fig. 5, it can be seen that due to its maximum transmittance over a broad spectral range (VIS and NIR), Si_3N_4 is a better antireflective coating than SiO_xN_y and SiO_2 , with an optical gain of the transmittance in the three basic colors in relation of these films to 11% and 24% in the blue color, 17% and 26% in the green color, and finally 9% and 17% in the red color, respectively.

FTIR measurements of all ARCs deposited by ECR-CVD show two doublets, with the characteristic absorption band of Si–H modes between 2235 and 2364 cm^{-1} . An important feature observed in the FTIR results is that the maximum peak of the SiO_xN_y (stretching 1008 cm^{-1}) is found between the two well known peaks reported in the literature for the SiO_2 and Si_3N_4 (1080 and 845.6 cm^{-1} , respectively). The observation of the stretching vibration mode at 1008 cm^{-1} in the spectrum indicates the presence of the Si–N bending in the SiN_xO_y films. The display of the sharp spectral band

obtained for our samples in the FTIR characterization reveals a high structural quality in the three ARCs, SiO_2 , Si_3N_4 , and SiO_xN_y .

VI. CONCLUSIONS

In this article, ARCs of SiO_2 , Si_3N_4 , and SiO_xN_y with several thicknesses have been fabricated and characterized. The refractive index and thickness measurements were compared using ellipsometry and interferometry techniques. The transmittance values show a very good agreement between the theoretical and experimental results. An optimized thickness that presents maximum transmittance for a broad spectral band on the VIS and NIR regions was determined for each ARC from simulations using MATHEMATICA program. A 60 nm thickness Si_3N_4 film was found to be the best ARC, presenting the highest transmittance over a broad spectral band. The sharp peaks in FTIR spectra indicate a highly uniform and excellent structural quality of the obtained ARCs. The process used is compatible with 2 μm CMOS technology.

ACKNOWLEDGMENTS

This work was financially supported by the Brazilian founding agencies Fundação de Amparo à Pesquisa do Estado de São Paulo (FAPESP) and Conselho Nacional de Desenvolvimento Científico e Tecnológico (CNPQ). The authors are grateful to Professor Dr. L. C. Barbosa and C. Lenz of the Universidade Estadual de Campinas for their kind permission for the use of their spectrophotometer.

- ¹M. White, D. Lampe, F. Blaha, and I. Mack, *IEEE J. Solid-State Circuits* **SC-9**, 1 (1974).
- ²M. Furumiya, H. Ohkubo, Y. Muramatsu, S. Kurosawa, F. Okamoto, Y. Fujimoto, and Y. Nakashiba, *IEEE Trans. Electron Devices* **48**, 2221 (2001).
- ³O. A. Popov and H. Waldron, *J. Vac. Sci. Technol. A* **7**, 914 (1989).
- ⁴O. S. Heavens, *Optical Properties of Thin Solid Films* (Dover, New York, 1991).
- ⁵V. M. Aroutiounian, K. R. Maroutyan, A. L. Zatikyan, and K. J. Touryan, *Thin Solid Films* **403**, 517 (2002).
- ⁶D. F. Edwards, in *Handbook of Optical Constants of Solids*, edited by E. D. Palik (Academic, Washington, D.C., 1985).
- ⁷M. L. Green, E. P. Gusev, R. Degraeve, and E. L. Garfunkel, *J. Appl. Phys.* **90**, 2057 (2001).
- ⁸M. I. Alayo, I. Pereyra, W. L. Scopel, and M. C. A. Fantini, *Thin Solid Films* **402**, 154 (2002).
- ⁹D. V. Tsu, G. Lucovsky, M. J. Mantini, and S. S. Chao, *J. Vac. Sci. Technol. A* **5**, 1998 (1987).
- ¹⁰G. Lucovsky, P. D. Richard, D. V. Tsu, S. Y. Lin, and J. Markunas, *J. Vac. Sci. Technol. A* **4**, 681 (1986).
- ¹¹E. A. Joseph, C. Gross, H. Y. Liu, R. T. Laaksonen, and F. G. Celii, *J. Vac. Sci. Technol. A* **19**, 2483 (2001).
- ¹²X. Wu, Ch. Ossadnik, Ch. Eggs, S. Veprek, and F. Phillipp, *J. Vac. Sci. Technol. B* **20**, 1368 (2002).
- ¹³J. A. Diniz, A. L. do Couto, I. Danilov, P. J. Tatsch, and J. W. Swart, *Proceedings of the XIV International Conference of Microelectronics and Packaging*, Faculty of Electrical and Computing Engineering, State University of Campinas, Brazil, 1999 (unpublished), p. 164.
- ¹⁴D. V. Tsu, G. Lucovsky, and M. J. Mantini, *Phys. Rev. B* **33**, 7069 (1986).
- ¹⁵C. M. M. Denisse, K. Z. Troost, J. B. Oude Elferink, F. H. P. M. Habraken, and W. F. van der Weg, *J. Appl. Phys.* **60**, 2536 (1986).